Journal of Solid State Chemistry **142,** 199–205 (1999)
Article ID jssc.1998.8035, available online at http://www.idealibrary.com on IDEAL®

Anomalous Thermoelectric Power Behaviors of Iodine Intercalated $(Bi,Pb)_2Sr_2Ca_{n-1}Cu_nO_{2n+4+\delta}$ Superconductors ($n = 2$ and 3)

J.-H. Choy,[1] S.-J. Hwang, and W. Lee

Department of Chemistry, Center for Molecular Catalysis, College of Natural Sciences, Seoul National University, Seoul 151-742, Korea

Received April 6; 1998; in revised form September 17, 1998; accepted September 21, 1998

Thermoelectric powers (TEPs) of the pristine $(Bi,Pb)_2Sr_2Ca_{n-1}Cu_nO_{2n+4+\delta}$ ($n=2$ and 3) compounds and their iodine intercalates were measured as a function of temperature, in order to investigate the effect of intercalation on the conduction mechanism of the host compounds. From the comparative measurements, it is revealed that the iodine intercalation gives rise to different evolution of TEP depending upon the host lattice, i.e., a downward shift for $Bi_2Sr_2CaCu_2O_{8+\delta}$ and an upward shift for $Bi_{2-x}Pb_xSr_2Ca_2Cu_3O_{10+\delta}$. In order to elucidate an origin of such contrasting TEP behaviors in both intercalates, the evolution of electronic structure upon intercalation has been examined by performing the systematic micro-Raman and X-ray absorption near edge structure (XANES) analyses. According to the Raman and I L_I-edge XANES studies, it is found that there is a partial electron transfer from host lattice to guest layer that is the same for both intercalates, which is in contrast with their opposite shifts of TEP. The present Cu K- and Bi L_{III}-edge XANES results also indicate the cooxidation of CuO_2 and BiO layers for both intercalates, whereas the Pb L_{III}-edge XANES analysis makes it clear that the Pb^{+IV} ion in $Bi_{2-x}Pb_xSr_2Ca_2Cu_3O_{10+\delta}$ is completely reduced to Pb^{+II} ion upon intercalation, leading to a decrease of hole contribution to TEP and consequently to an upward shift of TEP. From the present experimental findings, it becomes clear that a simple application of the universal plot of TEP (300 K) vs hole density may result in an inaccurate estimation of the oxidation state of CuO_2 layer. © 1999 Academic Press

INTRODUCTION

A growing realization that Bi-based cuprates are the appropriate host materials for intercalation reactions and the interest in Bi-based cuprates generated by our publication of high-T_c superconductors in the two-dimensional limit led to the investigation of the interactions of halogen molecular ions with Bi-based cuprate host lattices (1–10). In addition, intercalation reactions into high-T_c superconductors have been studied not only to investigate the mechanism responsible for high-T_c superconductivity but also to gain an understanding of the other physical properties of layered copper oxides (9, 10), since it provides an effective method for freely tuning the strength of interlayer coupling as well as controlling the hole density of CuO_2 layer. Among the transport properties of high-T_c superconducting oxides, intense research efforts have been devoted to understanding the thermoelectric power (TEP) of these materials (11–19). However, although the room temperature TEP has been widely used as a practical tool for determining the hole concentration in a CuO_2 plane (11), a complete and universal interpretation of this property has not yet been established. In the case of Bi- and Tl-based cuprates, TEP has also been believed to reflect accurately a change in hole density of a CuO_2 layer (12–14). The temperature dependence of TEP in these compounds has been explained by adopting the two-band model where TEP is strongly dependent upon the electronic structure near the Fermi level (E_F) (15–17). According to the band calculation for Bi-based cuprates (20, 21), it is found that the Bi 6*p* band contributes to the Fermi surface of these materials and its position is strongly dependent upon the structural distortion of the BiO layer. Since the intercalation into the Bi_2O_2 double layer of Bi-based cuprates would induce a significant modification of Bi electronic structure, it is expected to give an excellent opportunity for examining the applicability of two-band model to these materials. Moreover, because a charge transfer between host and guest upon intercalation leads to a change of oxidation state of a CuO_2 layer, the intercalation reaction allows us to probe the universality of the previously reported relationship between room temperature TEP and hole concentration of a CuO_2 layer (11). Finally, we can also investigate the influence of *c*-axis interlayer coupling on TEP of the layered superconductor, since the interlayer distance can be modified by the intercalation of guest molecules into superconducting layers (18).

In this study, an attempt has been made to measure the temperature-dependent TEP for the pristine $(Bi,Pb)_2Sr_2Ca_{n-1}Cu_nO_{2n+4+\delta}$ ($n = 2$ and 3) compounds and their iodine intercalates, in order to probe the effect of iodine

[1]To whom correspondence should be addressed. Fax: (82) 2-872-9864. E-mail: jhchoy@plaza.snu.ac.kr

0022-4596/99 $30.00

intercalation on TEP of Bi-based cuprates. The TEP data obtained have been analyzed by performing the curve fitting analysis based on a two-band model. The systematic micro-Raman and X-ray absorption spectroscopic (XAS) studies have also been carried out to examine the relationship between the electronic structure near E_F and TEP.

EXPERIMENTAL

The pristine $(Bi,Pb)_2Sr_2Ca_{n-1}Cu_nO_{2n+4+\delta}$ ($n = 2$ and 3) compounds were prepared by the conventional solid state reaction as previously described (22–24), and their iodine intercalates were synthesized by heating the vacuum sealed tube containing the pristine polycrystals with excess iodine ($P_I \cong 10$ atm) (6,7). The first-stage iodine intercalate of $Bi_2Sr_2CaCu_2O_{8+\delta}$ was easily obtained by heating at 180°C for 1 h, whereas the intercalation of iodine into $(Bi,Pb)_2Sr_2Ca_2Cu_3O_{10+\delta}$ could be realized by a prolonged heating at 150°C for 10 h.

The formation of the first-stage intercalates, $I(Bi,Pb)_2Sr_2Ca_{n-1}Cu_nO_{2n+4+\delta}$ ($n = 2$ and 3), was confirmed by both powder X-ray diffraction (XRD) and thermogravimetric analyses (TGA). From the least square fitting of (0 0 l) XRD reflections, the basal increment upon intercalation was determined to be 3.74 Å for $n = 2$ and 3.63 Å for $n = 3$, which correspond to the van der Waals diameter of the iodine atom (25, 26). To check their superconducting properties, the magnetic susceptibility was measured as a function of temperature with a SQUID magnetometer in a field of 20 Oe.

The temperature-dependent TEP was obtained by applying the standard differential method, where the temperature was monitored by a copper–constantan differential thermocouple attached to two copper blocks. In the present experimental setup, the sample was sandwiched between two copper blocks by using GE 7031 varnish to ensure good thermal contact. The accuracy of each TEP data point was determined to be ± 0.1 μV/K.

The micro-Raman measurement was carried out at room temperature by using a Jobin-Yvon/Atago Bussan T64000 triple spectrometer equipped with microoptics. The samples were excited with the 514.5-nm line of an Ar^+ laser. All the present spectra of the intercalates were obtained from the backscattering of the freshly fractured pellet surfaces. In order to prevent possible thermal damage of the samples, the power of incident laser light was maintained at less than 1 W. The resolution of present spectra was determined to be 3–4 cm^{-1}. All the Raman spectra measured at different areas of the fractured surface were found to be identical, indicating the homogeneity of the present samples.

The present XAS spectra were measured with synchrotron radiation by using the extended X-ray absorption fine structure (EXAFS) facilities installed at beam lines 7C and 10B at the Photon Factory in Tsukuba, operated at 2.5 GeV and 260–370 mA (27). The samples were finely ground, mixed with boron nitride (BN) in an appropriate ratio, and pressed into pellets in order to get the optimum absorption jump ($\Delta\mu t \approx 1$) needed to be free from the thickness and pin-hole effects (28). All the present spectra were obtained in a transmission mode using gas-ionization detectors. To ensure spectral reliability, much care has been taken to evaluate the stability of energy scale by monitoring the spectra of Cu metal and Bi_2O_3 for each measurement and thus the edge positions were reproducible to better than 0.05 eV. The inherent background in the data was removed by fitting a polynomial to the pre-edge region and extrapolated through the entire spectrum, from which it was subtracted. The resulting spectra, $\mu(E)$, were normalized to an edge jump of unity for comparing the XANES features directly with one another.

RESULTS AND DISCUSSION

According to the magnetic susceptibility measurements, the iodine intercalated $I(Bi,Pb)_2Sr_2Ca_{n-1}Cu_nO_{2n+4+\delta}$ ($n = 2$ and 3) compounds are found to have the high-T_c superconductivity with slightly lowered T_cs ($\Delta T_c = 10$ K) compared to those of the corresponding pristine compounds. Such T_c depressions upon iodine intercalation were already reported and interpreted as a result of a partial electron transfer from host lattice to guest layer (6, 25).

In order to investigate the effect of intercalation on the transport property of the host compound as well as on the hole concentration of a CuO_2 layer, we have measured the temperature-dependent TEP for the pristine $(Bi,Pb)_2Sr_2Ca_{n-1}Cu_nO_{2n+4+\delta}$ ($n = 2$ and 3) and its iodine intercalates (Fig. 1). All the present compounds exhibit an almost linear temperature dependence of TEP with a negative slope at $T > T_{max}$. As the temperature decreases, TEP increases, passes through a maximum, and then sharply drops to zero near T_c, except for $IBi_2Sr_2CaCu_2O_{8+\delta}$, which exhibits negative TEP values for the entire temperature region. Such a temperature dependence of TEP was already reported for Bi- and Tl-based cuprates with different hole concentrations (12–14). Although TEP of this material has been believed to be inversely proportional to the hole concentration of a CuO_2 layer (11), the iodine intercalation is revealed to have opposite influences on TEP depending upon the pristine compounds. That is, $Bi_2Sr_2CaCu_2O_{8+\delta}$ shows a downward shift of TEP upon intercalation, whereas $IBi_{2-x}Pb_xSr_2Ca_2Cu_3O_{10+\delta}$ exhibits TEP values higher than those of the pristine compound. Such an antipodal behavior in TEP upon intercalation suggests that there is a different direction of charge transfer depending upon the host lattice. However, taking into account the Lewis acidic character of iodine (29), an upward TEP shift of $IBi_{2-x}Pb_xSr_2Ca_2Cu_3O_{10+\delta}$, suggestive of a decrease in hole density, is considered to be anomalous. In this regard, we have

also monitored the evolution of TEP of $Bi_{2-x}Pb_xSr_2Ca_2Cu_3O_{10+\delta}$ after the same heat treatment in vacuum as used for the iodine intercalate, in order to check out the possibility of oxygen loss during intercalation reaction which may result in an upward shift of TEP. However, only a small increase of $\sim 1\,\mu V/K$ is observed after the heat treatment, showing that the oxygen loss during intercalation cannot account for the jump in TEP of $IBi_{2-x}Pb_xSr_2Ca_2Cu_3O_{10+\delta}$. Therefore, it is quite certain that the anomalous shift of TEP upon intercalation should be attributed mainly to an interaction between host and guest.

In order to get a detailed information on the electronic structure near E_F, curve-fitting analysis has been performed for the present TEP data by using a two-band model where a hole shows a metallic conduction and an electron has a semiconductor-like conduction mechanism (15–17). In this model, the temperature- dependent Seebeck coefficient (S) is expressed as

$$S = AT + (B\lambda + CT)\exp(-\lambda/T), \qquad [1]$$

where A, B, and C are the constants for a particular material, T is the temperature, λ is E_c/k, E_c is the energy measured from the center of band gap to the bottom of the conduction band, and k is the Boltzmann constant (15). The fitted data are compared with the experimental ones as shown in Fig. 1 and the obtained parameters are summarized in Table 1. For both the pristine materials, iodine intercalation induces a common increase in λ which is closely related with semiconducting band gap, indicating the similar effect of intercalation on the semiconductor-like conduction processes of both compounds. On the contrary, the constant A, inversely proportional to hole contribution, is found to decrease for $IBi_2Sr_2CaCu_2O_{8+\delta}$ but increase for $IBi_{2-x}Pb_xSr_2Ca_2Cu_3O_{10+\delta}$, which implies that iodine intercalation has different influences on the hole conduction process, depending on the host lattice. However, it is worth noting that the negative constant A of $IBi_2Sr_2CaCu_2O_{8+\delta}$, representing the positive hole contribution, is less physically meaningful, although the present fitting results are believed to provide reliable information on the effect of intercalation on each conduction mechanism.[2]

In order to clarify an origin of such anomalous variations of TEP caused by intercalation, we have performed the systematic micro-Raman and XAS studies for both pristine compounds and their intercalates. Figure 2 represents the

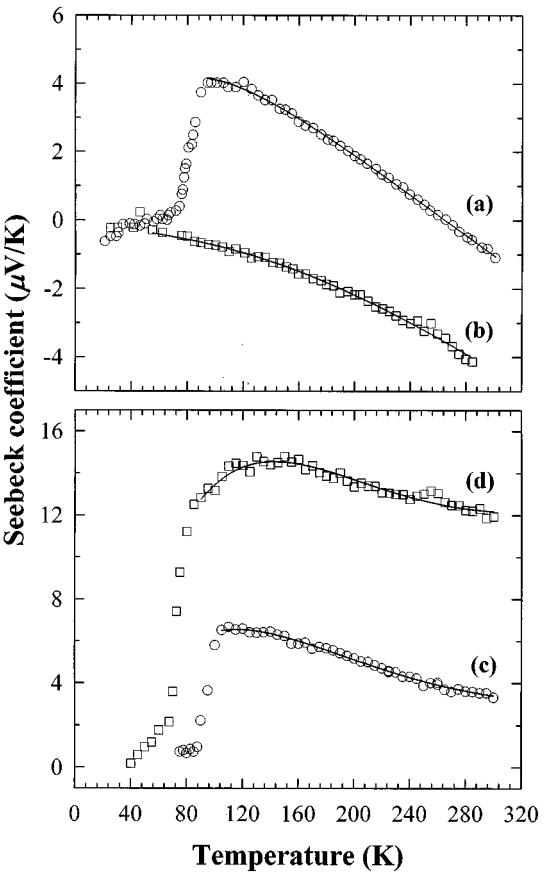

FIG. 1. Comparison of experimental Seebeck coefficients (S) with fitted ones for (a) $Bi_2Sr_2CaCu_2O_{8+\delta}$, (b) $IBi_2Sr_2CaCu_2O_{8+\delta}$, (c) $Bi_{2-x}Pb_xSr_2Ca_2Cu_3O_{10+\delta}$, and (d) $IBi_{2-x}Pb_xSr_2Ca_2Cu_3O_{10+\delta}$. The symbols and lines represent the experimental and calculated data, respectively.

micro-Raman spectra of $I(Bi,Pb)_2Sr_2Ca_{n-1}Cu_nO_{2n+4+\delta}$ ($n = 2$ and 3), which are also compared with those of the references KI_3 and I_2. The overall spectral features of both iodine intercalates are quite similar to that of the reference KI_3, suggesting the presence of triiodide ion (I_3^-). According to the previous assignment for CsI_3 (30), the strong peaks at ~ 105 and $\sim 145\ cm^{-1}$ can be attributed to the symmetric ν_1 and asymmetric ν_3 vibrations of I_3^- ion, respectively. The existence of triiodide species is further evidenced from the observation of $2\nu_1$ and $3\nu_1$ overtones around 215 and $320\ cm^{-1}$. Therefore, it becomes obvious that the intercalated iodine is stabilized as a negatively charged I_3^- ion in the interlayer space of both pristine compounds.

The I L_I-edge XANES spline and second derivative spectra for the iodine intercalates and some references are shown in Figs. 3a and 3b, respectively. All the present spectra except KI exhibit a characteristic pre-edge peak A around 5186 eV, which corresponds to the transition from core $2s$ level to $5p$ state above E_F. Since the intensity of this pre-edge peak is directly proportional to the density of the

[2] An attempt has been made to get a reasonable fitting result for $IBi_2Sr_2CaCu_2O_{8+\delta}$ by modifying the above relation as $S = A\cdot\exp(\lambda/T) + B\cdot\lambda/T + C$, based on the assumption that the electron in BiO layer plays a main role in thermoelectricity of this material. However, the modified equation gives only a poorer fit, implying that a simple assumption of two band structure is not applicable to the Bi-based cuprate with an overdoped hole density.

TABLE 1
The Best Fit Parameters, A, B, C, and λ of Eq. [1] and E_g Values Determined from λ for the Pristine $(Bi, Pb)_2Sr_2Ca_{n-1}Cu_nO_{2n+4+\delta}$ ($n = 2$ and 3) and Their Iodine Intercalates

Compound	A ($\mu V/K^2$)	B ($\mu V/K^2$)	C ($\mu V/K^2$)	λ(K)	E_g (eV)[a]
$Bi_2Sr_2CaCu_2O_{8+\delta}$	0.0782	− 0.0778	− 0.105	193	0.033
$IBi_2Sr_2CaCu_2O_{8+\delta}$	− 0.00689	7.62×10^{-5}	− 0.0285	390	0.067
$Bi_{2-x}Pb_xSr_2Ca_2Cu_3O_{10+\delta}$	0.0843	− 0.172	− 0.0324	344	0.059
$IBi_{2-x}Pb_xSr_2Ca_2Cu_3O_{10+\delta}$	0.161	− 0.306	− 0.0402	382	0.066

[a] These values are determined from the equation of $E_g = 2E_c = 2k\lambda$.

unoccupied I 5p final state, it reflects sensitively the oxidation state of the iodine species (31, 32). In this context, a remarkable decrease in the peak intensity for both intercalates with respect to free I_2 shows that there is a partial electron transfer from host lattice to iodine layer, which is well consistent with the present Raman results.

Figure 4a and 4b represent the Cu K-edge XANES spline and second derivative spectra for the pristine $(Bi,Pb)_2Sr_2Ca_{n-1}Cu_nO_{2n+4+\delta}$ ($n = 2$ and 3) and its iodine intercalates, respectively. All the observed fine features are identified as the dipole-allowed transitions from core 1s state to unoccupied 4p one, except for the pre-edge peak P corresponding to the quadrupole-allowed transition of $1s \rightarrow 3d$. According to our previous Cu K-edge XAS study (33), the main-edge peaks A and B are attributed to the transitions from 1s orbital to an out-of-plane $4p_\pi$ one with and without shakedown processes (34), respectively, whereas the features A′ and C are ascribed to the in-plane $4p_\sigma$ orbital transitions with and without shakedown processes. As shown in the second derivative spectra of Fig. 4b, the iodine intercalation induces a blue shift of edge position by 0.2 eV for $Bi_2Sr_2CaCu_2O_{8+\delta}$ and by 0.1 eV for $Bi_{2-x}Pb_xSr_2Ca_2Cu_3O_{10+\delta}$, respectively, indicating the slight oxidation of CuO_2 layer (35). Although such an increase of hole density seems to be contrasted with an upward shift of TEP for

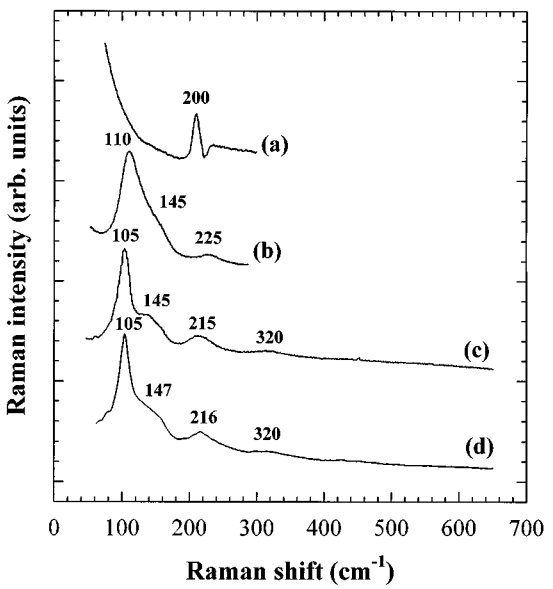

FIG. 2. Micro-Raman spectra of (a) I_2, (b) KI_3, (c) $IBi_2Sr_2CaCu_2O_{8+\delta}$, and (d) $IBi_{2-x}Pb_xSr_2Ca_2Cu_3O_{10+\delta}$.

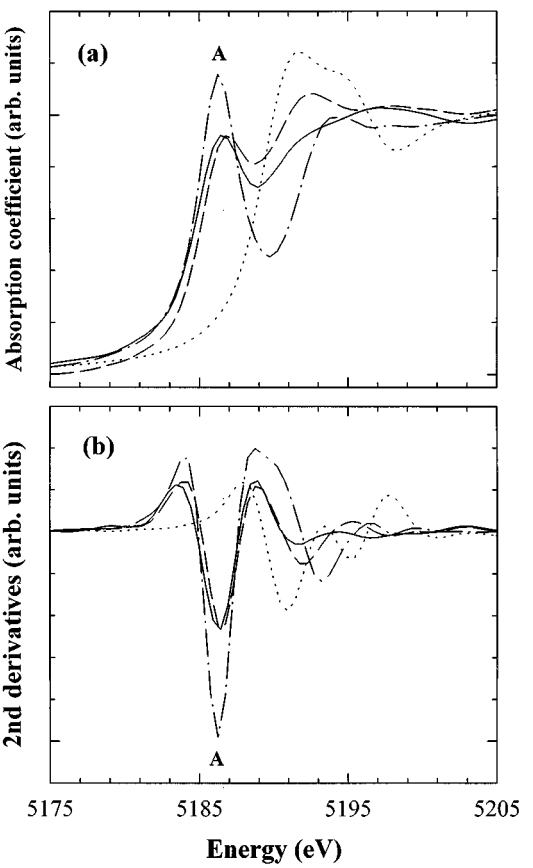

FIG. 3. I L_I-edge XANES (a) spline and (b) second derivative spectra for I_2 (dot-dashed lines), $IBi_2Sr_2CaCu_2O_{8+\delta}$ (solid lines), $IBi_{2-x}Pb_xSr_2Ca_2Cu_3O_{10+\delta}$ (dashed lines), and KI (dotted lines), respectively.

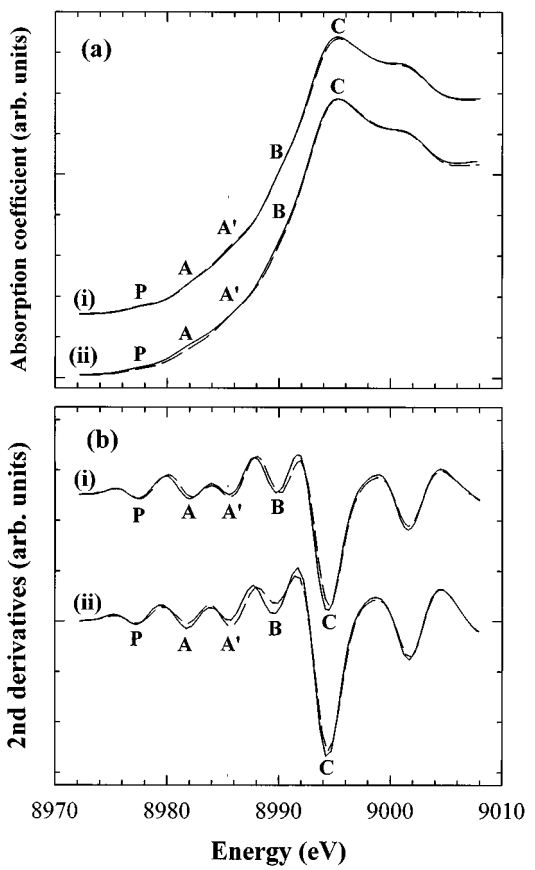

FIG. 4. Cu K-edge XANES (a) spline and (b) second derivative spectra for the pristine $(Bi,Pb)_2Sr_2Ca_{n-1}Cu_nO_{2n+4+\delta}$ and their iodine intercalates with (i) $n = 2$ and (ii) $n = 3$. The solid and dashed lines represent the spectra for pristine compounds and iodine intercalates, respectively.

$IBi_{2-x}Pb_xSr_2Ca_2Cu_3O_{10+\delta}$, the oxidation of CuO_2 layer upon intercalation is supported from the previous report where the T_c of $Bi_{2-x}Pb_xSr_2Ca_2Cu_3O_{10+\delta}$ with underdoped hole content is enhanced by intercalating iodine molecule (25).

The Bi L_{III}-edge XANES spline and second derivative spectra for the pristine $(Bi,Pb)_2Sr_2Ca_{n-1}Cu_nO_{2n+4+\delta}$ ($n = 2$ and 3) are represented in Figs. 5a and 5b, respectively, together with those for the corresponding iodine intercalates. It is clearly observed that the main edge position is shifted by 0.1–0.2 eV toward a high energy side upon intercalation, indicative of the oxidation of BiO layer. In addition to the edge shift, the iodine intercalation also leads to a decrease in the energy difference between the peaks B and C, corresponding to the $2p_{3/2} \rightarrow 6d_{t_{2g}}$ and $2p_{3/2} \rightarrow 6d_{e_g}$ transitions, respectively (36, 37), which is due to the weakening of the crystal field around Bi upon intercalation (38). This is well consistent with the oxidation of CuO_2 layer, which results in a decrease of $(Cu–O_{Sr})$ bond distance and, in turn, an elongation of the competing $(Bi–O_{Sr})$ one (6).

Figures 6a and 6b represent the Pb L_{III}-edge XANES spectra and their second derivatives for the pristine $Bi_{2-x}Pb_xSr_2Ca_2Cu_3O_{10+\delta}$ and its iodine intercalate, respectively, those which are also compared with those for the reference PbO. Since the pristine compound has a mixed Pb oxidation state of Pb^{+IV}/Pb^{+II} with the vacant 6*s* and 6*d* orbitals (39), not only the main-edge peaks B and C corresponding to the $2p_{3/2} \rightarrow 6d_{t_{2g}}$ and $2p_{3/2} \rightarrow 6d_{e_g}$ transitions but also the pre-edge peak A corresponding to the $2p_{3/2} \rightarrow 6s$ one can be observed for this compound (40). The peak A is also detected for the reference PbO, even though this compound has the formal oxidation state of Pb^{+II} with a fully occupied 6*s* orbital. However, in this case, this feature is ascribed to a transition to an unoccupied *p–d* hybridized level, not to 6*s* level (41). Like the Bi L_{III}-edge XANES spectra, the energy difference between peaks B and C decreases upon intercalation, which also signals a weakening of the crystal field around Pb. In addition to such small shifts of spectral features, the iodine intercalation also induces more significant changes in Pb L_{III}-edge XANES spectra, namely, a complete disappearance of the pre-edge peak

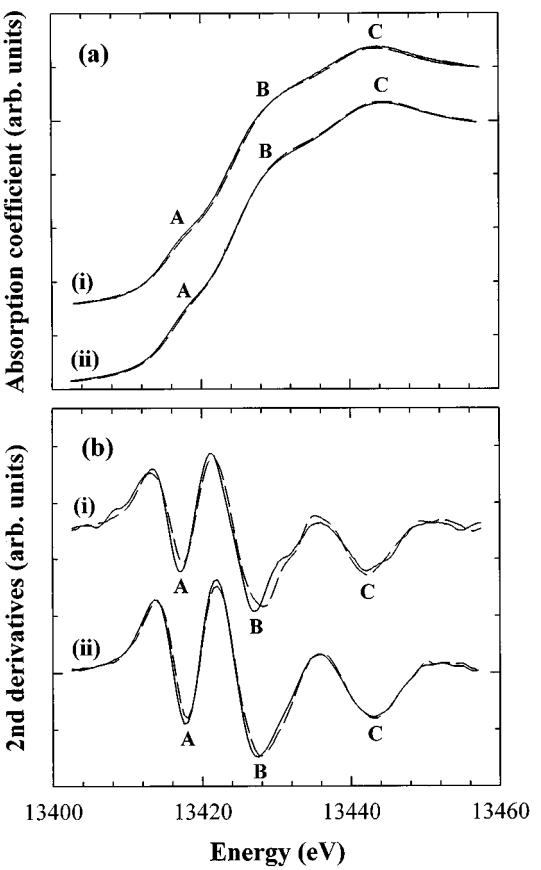

FIG. 5. Bi L_{III}-edge XANES (a) spline and (b) second derivative spectra for the pristine $(Bi,Pb)_2Sr_2Ca_{n-1}Cu_nO_{2n+4+\delta}$ and their iodine intercalates with (i) $n = 2$ and (ii) $n = 3$. The solid and dashed lines represent the spectra for pristine compounds and iodine intercalates, respectively.

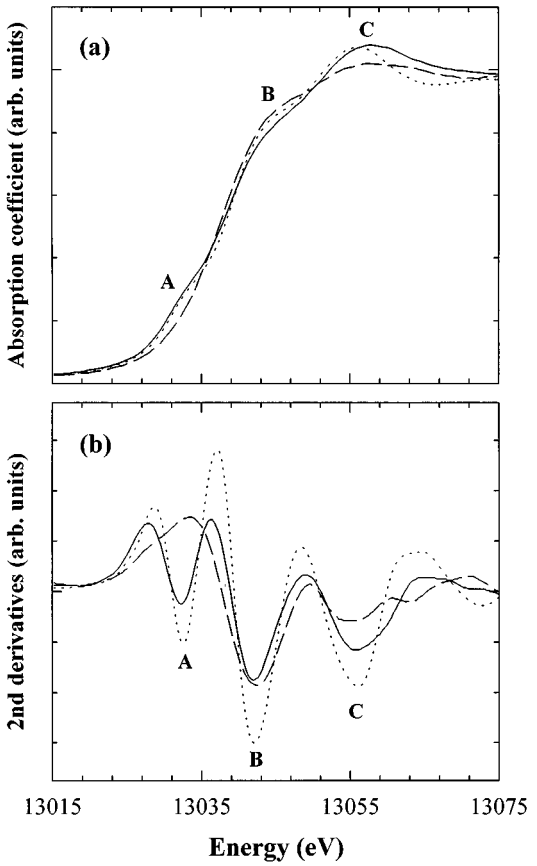

FIG. 6. Pb L_{III}-edge XANES (a) spline and (b) second derivative spectra for $Bi_{2-x}Pb_xSr_2Ca_2Cu_3O_{10+\delta}$ (solid lines), $IBi_{2-x}Pb_xSr_2Ca_2Cu_3O_{10+\delta}$ (dashed lines), and PbO (dotted lines).

A and a remarkable downward shift of the main edge. These findings provide clear evidence of the complete reduction of a Pb^{+IV} ion into a Pb^{+II} one upon intercalation, implying that the Pb 6*s* band does not contribute to Fermi surface of $IBi_{2-x}Pb_xSr_2Ca_2Cu_3O_{10+\delta}$. Such an evolution of the Pb oxidation state is expected to be achieved through the charge transfer between Pb and Cu and/or Pb and Bi, as already suggested from the previous XANES study on the Pb-substituted Bi-based cuprates (40). Taking into account a remarkable decrease of hole contribution to TEP of $Bi_{2-x}Pb_xSr_2Ca_2Cu_3O_{10+\delta}$ upon intercalation, it is thought that the holes in the Pb 6*s* band contribute to the thermoelectricity of this compound and the reduction of Pb^{+IV} ion results in the extinction of hole contribution from Pb. In fact, such a coexistence of two different charge carriers in the same Bi(Pb)O plane has been already suggested for $BaBi_{0.25}Pb_{0.75}O_3$, on the basis of TEP measurement and band calculation (42, 43). On the other hand, since the Pb 6*s* band is much dispersed than the Cu 3*d* one, the hole mobility is considered to be higher for the former. Moreover, the metallization of Bi(Pb)O layer upon iodine intercalation would increase the contribution of this layer to the TEP of iodine intercalates (10). For this reason, the elimination of holes in the Pb 6*s* band leads to a net upward shift of TEP upon intercalation, in spite of a slight increase of hole density in CuO_2layer.

On the other hand, based on the recent report where the TEP of high-T_c superconductors is inversely proportional to the strength of interlayer coupling (18), an attempt has also been made to explain such an anomalous TEP shift upon intercalation by considering a change of interlayer coupling. Since the substitution of Bi with Pb enhances remarkably the interaction between the superconducting blocks, $Bi_{2-x}Pb_xSr_2Ca_2Cu_3O_{10+\delta}$ is expected to have much stronger coupling strength than $Bi_2Sr_2CaCu_2O_{8+\delta}$ (44). In this context, the increment of TEP for $IBi_{2-x}Pb_xSr_2Ca_2Cu_3O_{10+\delta}$ might be attributed to a more prominent depression of interlayer coupling upon intercalation than seen with $IBi_2Sr_2CaCu_2O_{8+\delta}$ (18). However, according to the recent TEP measurement for mercuric iodide intercalated $Bi_{2-x}Pb_xSr_2Ca_2Cu_3O_{10+\delta}$ whose basal spacing is much larger than that of iodine intercalate, the TEP increase upon intercalation is revealed to be less prominent for the HgI_2 intercalate than for the iodine one,[3] even though the interlayer coupling along *c*-axis should be weaker for the former than for the latter. Therefore, it can be concluded that an upward shift of TEP for the iodine intercalated $Bi_{2-x}Pb_xSr_2Ca_2Cu_3O_{10+\delta}$ is mainly originated from a modification of Pb electronic structure rather than from a weakening of interlayer coupling.

CONCLUSION

In this work, we have investigated the effect of iodine intercalation on the temperature-dependent TEP of the pristine $(Bi,Pb)_2Sr_2Ca_{n-1}Cu_nO_{2n+4+\delta}$ ($n = 2$ and 3) compounds. Although both the host materials exhibit the different evolution of TEP upon intercalation, suggestive of opposite directions in charge transfer, the present XAS and micro-Raman results indicate that there is a partial electron transfer from host lattice to guest layer that is common for both the iodine intercalates. On the other hand, the Pb L_{III}-edge XANES analysis reveals that the tetravalent Pb^{+IV} ion in (Bi,Pb–O) layer of $Bi_{2-x}Pb_xSr_2Ca_2Cu_3O_{10+\delta}$ is fully reduced to the Pb^{+II} ion by intercalating iodine molecules, leading to a decrease of highly mobile hole carriers in this layer. In this respect, we have interpreted an upward shift of TEP for $IBi_{2-x}Pb_xSr_2Ca_2Cu_3O_{10+\delta}$ as a result of an extinction of holes in the Pb 6s band. From the present experimental findings, it becomes obvious that a caution should be exercised on an application of the universal plot of TEP vs hole density to determine the oxidation state of CuO_2 layer.

[3] The detailed synthesis and characterization of mercuric iodide intercalated $Bi_{2-x}Pb_xSr_2Ca_2Cu_3O_{10+\delta}$ will be published elsewhere.

ACKNOWLEDGMENTS

This work was supported in part by the Ministry of Education (BSRI-97-3413) and by the Korean Science and Engineering Foundation through the Center for Molecular Catalysis. Our thanks are extended to Prof. Y. W. Park for TEP measurements.

REFERENCES

1. J.-H. Choy, N.-G. Park, S.-J. Hwang, D.-H. Kim, and N. H. Hur, *J. Am. Chem. Soc.* **116,** 11564 (1994).
2. J.-H. Choy, S.-J. Hwang, and N.-G. Park, *J. Am. Chem. Soc.* **119,** 1624 (1997).
3. J.-H. Choy, N.-G. Park, S.-J. Hwang, and Z.-G. Khim, *J. Phys. Chem.* **100,** 3783 (1996).
4. J.-H. Choy, N.-G. Park, Y.-I. Kim, J. S. Lee, and H. I. Yu, *J. Phys. Chem.* **99,** 2157 (1993).
5. J.-H. Choy, S.-J. Kwon, and G.-S. Park, *Science* **280,** 1589 (1998).
6. S.-J. Hwang, N.-G. Park, D.-H. Kim, and J.-H. Choy, *J. Solid State Chem.* **138,** 66 (1998).
7. Y.-S. Song, Y.-S. Ha, C.-S. Whang, Y.-W. Park, M. Itoh, S.-G. Kang, S.-J. Hwang, and J.-H. Choy, *in* "Superconducting Materials" (J. Etourneau, J.-B. Torrance, and H. Yamauchi Eds.), p. 323. IITT-International, Paris, 1993.
8. X.-D. Xiang, S. McKernan, W. A. Vareka, A. Zettl, J. L. Corkill, T. W. Barbee III, and M. L. Cohen, *Nature* **332,** 145 (1990).
9. M.-K. Bae, M.-S. Kim, S.-I. Lee, J.-H. Choy, N.-G. Park, S.-J. Hwang, and D.-H. Kim, *Phys. Rev.* B **53,** 12416 (1996).
10. X.-D. Xiang, W. A. Vareka, A. Zettl, J. L. Corkill, and M. L. Cohen, *Phys. Rev. Lett.* **68,** 530 (1992).
11. S. D. Obertelli, J. R. Cooper, and J. L. Tallon, *Phys. Rev.* B **46,** 14928 (1992).
12. J. B. Mandel, S. Keshi, P. Mandel, A. Poddar, A. N. Das, and B. Ghosh, *Phys. Rev.* B **46,** 11840 (1992).
13. C. R. Varoy, H. J. Trodahl, F. G. Buckley, and A. B. Kaiser, *Phys. Rev.* B **46,** 463 (1992).
14. S. Keshi, J. B. Mandel, P. Mandel, A. Poddar, A. N. Das, and B. Ghosh, *Phys. Rev.* B **47,** 9048 (1993).
15. Y. Xin, K. W. Wong, C. X. Fan, Z. Z. Sheng, and F. T. Chan, *Phys. Rev.* B **48,** 557 (1993).
16. V. P. S. Awana, V. N. Moorthy, and A. V. Narlikar, *Phys. Rev.* B **49,** 6385 (1994).
17. B. Chanda, S. K.Ghatak, and T. K. Dey, *Physica* C **232,** 136 (1994).
18. J. S. Zhou and J. B. Goodenough, *Phys. Rev.* B **54,** 12488 (1996).
19. L. Forro, J. Lukatela, and B. Keszei, *Solid State Commun.* **73,** 501 (1990).
20. W.-E. Pickett, *Rev. Mod. Phys.* **61,** 433 (1989).
21. L.-F. Mattheiss and D.-R. Hamann, *Phys. Rev.* B **38,** 5012 (1988).
22. J. M. Tarascon, W. R. McKinnon, P. Barboux, D. M. Hwang, B. G. Bagley, L. H. Greene, G. W. Hull, Y. Lepage, N. Stoffel, and M. Giroud, *Phys. Rev.* B **38,** 8885 (1988).
23. J.-H. Choy, S.-J. Kim, J.-C. Park, F. K. Frohlich, P. Dordor, and J. C. Grenier, *Bull. Kor. Chem. Soc.* **11,** 654 (1990).
24. The nominal compositions of the pristine compounds are $Bi_2Sr_{1.5}Ca_{1.5}Cu_2O_{8+\delta}$ for $n = 2$ and $Bi_{1.85}Pb_{0.35}Sr_{1.9}Ca_{2.1}Cu_{3.1}O_{10+\delta}$ for $n = 3$, respectively.
25. D. Pooke, K. Kishio, T. Kota, Y. Fukuda, N. Sandana, M. Nagoshi, K. Kitazawa, and K. Yamafuji, *Physica* C **198,** 349 (1992).
26. X.-D. Xiang, A. Zettl, W. A. Vareka, J. L. Corkill, T. W. Barbee III, and M. L. Cohen, *Phys. Rev.* B **43,** 11496 (1991).
27. H. Oyanagi, T. Matsushida, M. Ito, and H. Kuroda, *KEK Rep.* **83,** 30 (1984); H. Kuroda and A. Koyama, *KEK Rep.* **84,** 19 (1989).
28. F. W. Lytle, G. van der Laan, R. B. Greegor, E. M. Larson, C. E. Violet, and J. Wong, *Phys. Rev.* B **41,** 8955 (1990); E.-A. Stern and K. Kim, *Phys. Rev.* B **23,** 3781 (1981).
29. J. E. Huheey, E. A. Keiter, and R. L. Keiter, "Inorganic Chemistry," p. 347. HarperCollins College, New York, 1993.
30. W. Gabes and H. Gerding, *J. Mol. Struct.* **14,** 267 (1972).
31. N.-G. Park, S.-W. Cho, S.-J. Kim, and J.-H. Choy, *Chem. Mater.* **8,** 324 (1996).
32. J. E. Hahn, R. A. Scott, K. O. Hodgson, S. Doniach, S. R. Desjardins, and E. I. Solomon, *Chem. Phys. Lett.* **88,** 595 (1982).
33. J.-H. Choy, D.-K. Kim, S.-H. Hwang, and G. Demazeau, *Phys. Rev.* B **50,** 16631 (1994).
34. R. A. Bair and W. A. Goddard III, *Phys. Rev.* B **22,** 2767 (1980); N. Kosugi, H. Kondoh, H. Tajima, and H. Kuroda, *Chem. Phys.* **135,** 149 (1980).
35. The different degrees of edge shift for both compounds can be explained by the dissimilar number of CuO_2 layer in the unit block (two for $Bi_2Sr_2CaCu_2O_{8+\delta}$ and three for $Bi_{2-x}Pb_xSr_2Ca_2Cu_3O_{10+\delta}$). That is, the amount of hole doping per CuO_2 layer becomes smaller as the number of the layers increases.
36. F. Studer, D. Bourgault, C. Martin, R. Retoux, C. Michael, B. Raveau, E. Dartyge, and A. Fontaine, *Physica* C **159,** 609 (1989).
37. R. Retoux, F. Studer, C. Michael, B. Raveau, A. Fontaine, and E. Dartyge, *Phys. Rev.* B **41,** 193 (1990).
38. J.-H. Choy, D.-K. Kim, S.-H. Hwang, G. Demazeau, and D. Y. Jung, *J. Am. Chem. Soc.* **117,** 8557 (1995).
39. K. K. Liu, S. X. Dou, K.-H. Song, C. C. Sorrel, K. A. Easterling, and W. K. Jones, *J. Solid State Chem.* **87,** 289 (1990).
40. N. Merrien, F. Studer, G. Poullain, C. Michel, A. M. Flank, P. Lagarde, and A. Fontaine, *J. Solid State Chem.* **105,** 112 (1993).
41. K. J. Rao and *J. Wong*, *J. Chem. Phys.* **81,** 4832 (1984).
42. T. Hashimoto, R. Hirasawa, T. Yoshida, Y. Yonemura, J. Mizusaki, and H. Tagawa, *Phys. Rev.* B **51,** 576 (1995)
43. L. F. Mattheiss and D. R. Hamann, *Phys. Rev.* B **28,** 4227 (1983); L. F. Mattheiss and D. R. Hamann, *Phys. Rev.* B **26,** 2686 (19832.
44. C. S. Gopinath and S. Subramanian, *Physica* C **176,** 331 (1991); G.Calestani, M. G. Francesconi, G. Salsi, G. D. Andreetti, and A. Migliori, *Physica* C **197,** 283 (1993).